LARGE-SCALE FLOW STRUCTURE IN TURBULENT NONPREMIXED FLAMES UNDER NORMAL- AND LOW-GRAVITY CONDITIONS

N. T. Clemens, C. A. Idicheria and I. G. Boxx

Department of Aerospace Engineering & Engineering Mechanics, The University of Texas at Austin, Austin, TX 78712-1085

INTRODUCTION

It is well known that buoyancy has a major influence on the flow structure of turbulent nonpremixed jet flames. Buoyancy acts by inducing baroclinic torques, which generate large-scale vortical structures that can significantly modify the flow field. Furthermore, some suggest that buoyancy can substantially influence the large-scale structure of even nominally momentum-dominated flames, since the low velocity flow outside of the flame will be more susceptible to buoyancy effects.[1] Even subtle buoyancy effects may be important because changes in the large-scale structure affects the local entrainment and fluctuating strain rate, and hence the structure of the flame. Previous studies that have compared the structure of normal- and micro-gravity nonpremixed jet flames note that flames in microgravity are longer and wider than in normal-gravity.[2-5] This trend was observed for jet flames ranging from laminar to turbulent regimes. Furthermore, imaging of the flames has shown possible evidence of helical instabilities and disturbances starting from the base of the flame in microgravity. In contrast, these characteristics were not observed in normal-gravity.

The objective of the present study is to further advance our knowledge of the effects of weak levels of buoyancy on the structure of transitional and turbulent nonpremixed jet flames. In later studies we will utilize the drop tower facilities at NASA Glenn Research Center (GRC), but the preliminary work described in this paper was conducted using the 1.25-second drop tower located at the University of Texas at Austin. A more detailed description of these experiments can be found in Idicheria *et al.*[6]

EXPERIMENTAL APPARATUS/CONDITIONS

The experiments were conducted using a newly constructed jet flame drop-rig (Fig. 1) that is housed in a standard GRC 2.2 second droptower frame (38"x36"x16"). Piloted ethylene jet flames were studied, which issued from a 1.75 mm straight tube into quiescent air within the drop box. A premixed methane-air pilot flame was used to ignite the flame and to further forestall flame liftoff. The ethylene and methane were stored in two onboard, 18.3 in^3 stainless steel pressure vessels. Flow rates were controlled with line pressure regulators upstream of choked micro-metering valves. Line pressures were recorded using pressure transducers installed upstream of the micro-metering valves and read into the onboard computer. Solenoid valves, connected via solid-state relays to the digital I/O card of an onboard computer, were used to start and stop the flow. The onboard computer was a ruggedized Pentium Celeron based PC equipped with frame grabber and data acquisition cards. Flame luminosity was imaged using a progressive scan CCD camera (Pulnix TM-6710) operated at a resolution of 512x145 pixel^2 and 350 frames per second.

The preliminary data reported here were obtained with the 1.25-second drop tower at the University of Texas at Austin. The tower is 35 ft tall, with an 8 ft x 8 ft cross-section and provides a drop distance of 25 ft. The box is decelerated by falling into a 6 ft x 4 ft x 7 ft container filled with polyurethane foam cubes. Accelerometer data taken during the drops show

that low-gravity levels of 10-30 mg can be achieved. These relatively high g-levels result from the fact that no drag shield was used. The deceleration levels at impact were about 25g.

Jet flames at a range of Reynolds numbers were studied as shown in Table 1. The Reynolds number ($Re_D=U_0D/\nu$) is based on the jet exit diameter D, jet exit velocity U_0 and the kinematic viscosity of ethylene at room temperature. Also shown in Table 1 is

Table 1. Flow conditions.

Case	Fuel	U_0(m/s)	Re_D	ξ_L(1g)	ξ_L(20mg)
1	Ethylene	12.4	2,500	8.5	2.4
2	Ethylene	24.8	5,000	6.6	1.5
3	Ethylene	37.2	7,500	4.6	1.3
4	Ethylene	52.2	10,500	3.7	1.0

the parameter ξ_L, which was used by Becker and Yamazaki[7] to quantify the effect of buoyancy on the mean entrainment of turbulent jet flames. This buoyancy parameter is defined as $\xi_L=Ri_s^{1/3}L_f/D_s$, where Ri_s is the source Richardson number ($Ri_s=gD_s/U_s^2$) based on the source diameter $D_s=D(\rho_0/\rho_\infty)^{1/2}$, and source velocity $U_s=U_0$ for a top-hat velocity profile. L_f is the average visible flame length, g is the acceleration due to gravity, ρ_0 is the jet fluid density and ρ_∞ is the ambient density. Becker and Yamazaki[8] suggest that flames with $\xi_L<1$ are momentum dominated. Interestingly, this table shows that even under our milli-g conditions, the lower Reynolds number flames may exhibit some buoyancy effects.

RESULTS AND DISCUSSION

Figure 2 shows sample image sequences of the flame startup for low- and normal-gravity conditions at an exit Reynolds number of 7500. The jet was started only after the drop was initiated. The time to reach steady state was investigated quantitatively by analyzing the instantaneous flame tip location as a function of time. Figure 3 shows the flame length variation with time (as obtained from individual frames) for different Reynolds numbers. From these plots it is clearer that the low-gravity flame takes a longer time to reach steady state. Even in the low Reynolds number cases (2500 and 5000), the difference is only about 200 ms. At the higher Reynolds numbers, the startup transient is nearly the same for normal- and low-g, as the difference is about 100 ms. Also, in all cases the flame is seen to reach a steady state in less than 300 ms.

Figure 4 shows sample steady state sequences for a Reynolds number of 7500. The low-gravity sequence shows what appears to be evidence of a helical large-scale instability in agreement with Ref. 3, but a similar structure is not seen at 1g. The steady state sequences were used to compute mean emission images, as shown in Fig. 5, and from these the mean visible flame length (L_f) was measured. In all of the cases studied, there is little difference in the average visible flame lengths measured under normal- and low-gravity conditions, as shown in Figure 6. The maximum difference was of about 10% of the flame height at $Re_D=5,000$. Any differences in length and width between flames in normal- and low-gravity conditions are seen to diminish as the flame becomes more momentum dominated.

We also investigated the evolution of the large-scale structures in the flames using volume rendering of image sequences. This technique, discussed by Mungal et al.[8], gives good visual information on the structure evolution. In this technique a sequence of two-dimensional images (x-y) is stacked one behind the other along the z-axis (time, t) and a three dimensional volume (x-y-t) is generated. The surface of this 3-D model is an isocontour corresponding to the visible flame edge in each image. Volume rendering highlights features that are not immediately

apparent in the still images or movie sequences. Sample renderings at $Re_D=2500$ are shown in Figure 7. In these images, convection of large-scale structures appears as wrinkles traveling up and to the right on the surface of the volume. The slope of these wrinkles can be used as a qualitative estimate of the large-scale structure convection velocity. It can be seen that the flame tip in low-gravity (figure 7a) fluctuates at a lower frequency than in normal-gravity (figure 7b); however, in the higher Reynolds number case (figures not presented due to lack of space) we observed that the flame tip oscillations and large-scale structure convection velocities become comparable. All of these observations show the decreasing effect buoyancy has on flame characteristics and behavior, as ξ_L decreases.

FUTURE WORK

Our future work will be directed at investigating these observations further by utilizing the 2.2 second drop-tower at NASA GRC, which will provide us with purely momentum dominated flames in lower Reynolds numbers. We are also currently working on implementing laser-based diagnostics including Mie scattering and particle image velocimetry to further investigate the large-scale structures and strain-vorticity fields.

ACKNOWLEDGEMENTS

REFERENCES

1. Roquemore, W.M., Chen, L.D., Goss, L.P. and Lynn, W.F., Lecture notes in Engineering Vol. 40, Springer-Verlag, pp. 49-63 (1989).
2. Bahadori, M.Y., Stocker, D.P., Vaughan, D.F., Zhou, L. and Edelman, R.B., Modern Developments in Energy, Combustion and Spectroscopy, Pergamon Press, pp. 49-66.
3. Hegde, U., Yuan, Z.G., Stocker, D.P. and Bahadori, M.Y., AIAA paper 2000-0697 (2000).
4. Hegde, U., Yuan, Z.G., Stocker, D.P. and Bahadori, M.Y., Fifth International Microgravity combustion Workshop, May (2000).
5. Hegde, U., Zhou, L., Bahadori, M. Y., Combustion Science & Technology, Vol. 102, pp. 95-113 (1994).
6. Idicheria, C.A., Boxx, I.G. and Clemens, N.T., AIAA paper 2001-0628 (2001).
7. Becker, H. A. and Yamazaki, S., Combustion and Flame, Vol. 33, pp. 123-149 (1978).
8. Mungal, M.G., Karasso, P.S. and Lozano, A., Combustion Science & Technology, Vol. 76, pp. 165-185 (1991).
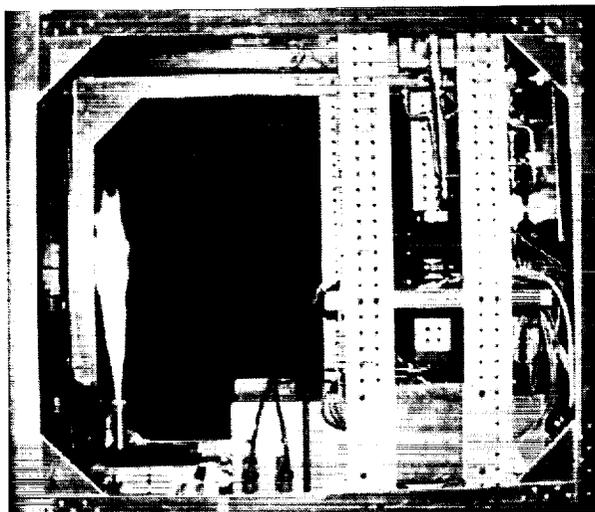
Figure 1. Photograph of the drop rig.

a) Re$_D$=7500, Low-gravity   b)Re$_D$=7500, Normal-gravity

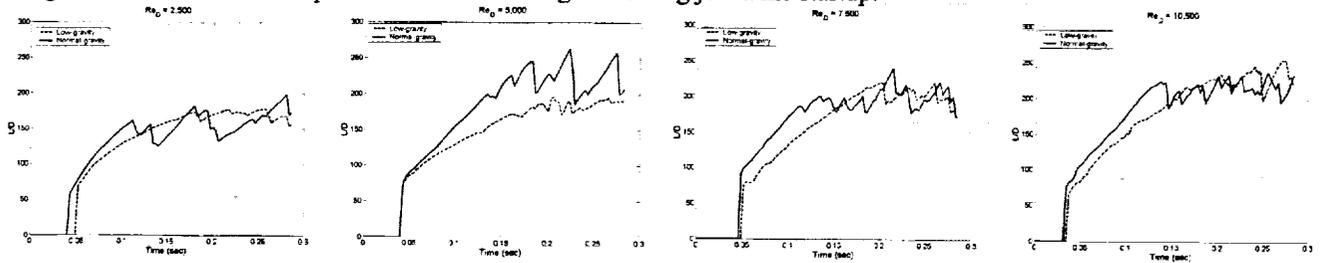Figure 2. Time resolved sequence of emission images showing jet-flame startup.

Figure 3. Flame tip variation with time for the various Reynolds numbers.

a) Re$_D$=7500, Low-gravity   b)Re$_D$=7500, Normal-gravity

Figure 4. Steady state sequences

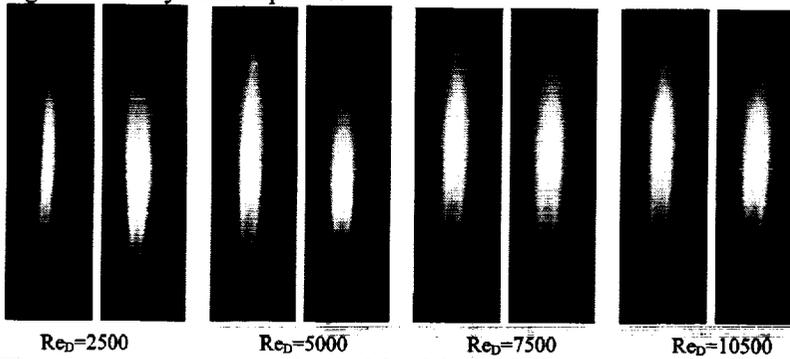Re$_D$=2500   Re$_D$=5000   Re$_D$=7500   Re$_D$=10500

Figure 5. Average images obtained for different Reynolds numbers. In each pair normal-gravity image is to the left and low-gravity image is to the right.
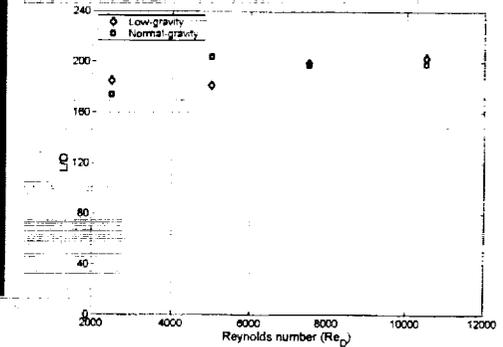
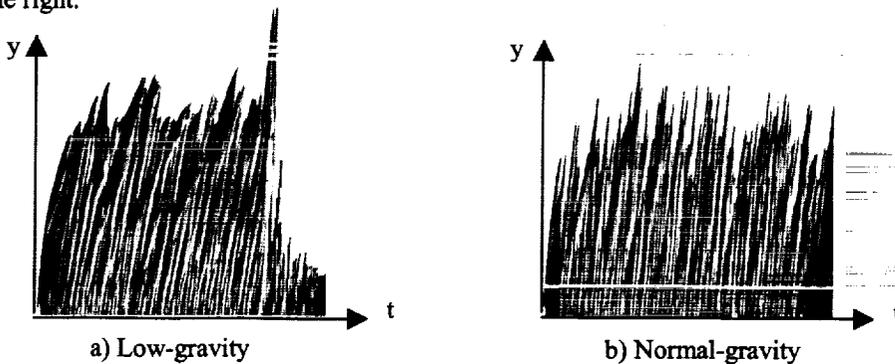Figure 6. Variation of flame height with Reynolds number.

a) Low-gravity   b) Normal-gravity

Figure 7. Sample volume renderings at Re$_D$=2500.